Manuscript for: *Journal of Materials Chemistry A*

J. Roosen, K. Binnemans
Journal of Materials Chemistry A 2, 1530–1540 (2014).

Adsorption and chromatographic separation of rare earths with EDTA- and DTPA-functionalized chitosan biopolymers

Joris Roosen and Koen Binnemans*

KU Leuven, Department of Chemistry, Celestijnenlaan 200F, P.O. Box 2404, B-3001 Heverlee (Belgium).

* Corresponding author:

E-mail: Koen.Binnemans@chem.kuleuven.be

Phone: +32 16 32 7446

Fax: +32 16 32 7992

Abstract

Chitosan, which is derived from chitin by deacetylation, is one of the most promising biopolymers for adsorption of metal ions from diluted waste streams. By functionalization of chitosan with ethylenediaminetetraacetic acid (EDTA) or diethylenetriaminepentaacetic acid (DTPA) groups, it is possible to obtain a material that is much less soluble in acidic aqueous solutions than native chitosan. The coordinating EDTA and DTPA ligands are very efficient for binding of rare-earth (lanthanide) ions. The functionalization was achieved by reaction of chitosan with EDTA bisanhydride or DTPA bisanhydride. The binding of lanthanide ions to functionalized chitosan was investigated by FTIR (binding of Nd^{3+}) and luminescence spectroscopy (binding of Eu^{3+}). Comparison of the luminescence decay times of the europium(III)-EDTA-chitosan complex swollen in water and in heavy water showed that four water molecules are coordinated to the Eu^{3+} ion. Batch adsorption tests for the uptake of neodymium(III) from aqueous nitrate solutions were performed for EDTA-chitosan and DTPA-chitosan. Different experimental parameters such as the adsorption kinetics, loading capacity and pH of the aqueous feed were investigated. The modified chitosan materials are much more effective for adsorption of rare earths than unmodified chitosan. It was shown that adjustment of the pH of the aqueous feed solution allows achieving selectivity for adsorption of rare-earth ions for mixtures with two different ions present. After stripping of the metal content, the modified chitosans could be reused for new adsorption experiments. Medium pressure liquid chromatography (MPLC) with DTPA-chitosan/silica as stationary phase and a dilute nitric acid solution as eluent was used for the separation of the following mixtures of rare-earth ions: Nd^{3+}/Ho^{3+}, Pr^{3+}/Nd^{3+} and $Pr^{3+}/Nd^{3+}/Ho^{3+}$. The experiments show that separation of the rare-earth ions is feasible with DTPA-chitosan/silica, without the need of using solutions of chelating agents as eluents.

Introduction

Removal of heavy metals from dilute aqueous waste streams is an important issue, due to the toxicity of metals such as cadmium, mercury or lead.[1,2] However, these waste streams can also contain valuable metals such as platinum-group metals (PGMs), silver, gold, gallium, indium and the rare-earth elements (REEs).[3] Recovery of these metal values from dilute aqueous streams could complement the supply of these metals from primary mining or recycling of end-of-life consumer goods.[4,5] Not only industrial aqueous waste streams could be considered, but also acid mine drainage (AMD) from metal or coal mines.[6] These methods for the recovery of metals can also be applied to the winning of metals from seawater. Earlier attempts to extract gold from seawater were not successful,[7] but recent Japanese studies showed that many metals, including uranium, can be obtained from seawater.[8,9]

Recovery of metals from *dilute aqueous streams* should be done by ion exchange or chelating resins, not by solvent extraction.[10,11] Solvent extraction is very suitable for separation of metals in high concentrations, but not from diluted aqueous streams, because the risk of contamination of the aqueous streams by organic solvents and extractants is too large. Although commercially available ion-exchange resins and chelating resins (e.g. Chelex® 100) are able to sequester metal ions from aqueous solutions, they suffer from low loading capacities and they are often very expensive. Therefore, the search for low-cost adsorbents for metal ions is a very active research field.[12-14] Different inorganic and organic adsorbents have been tested. Examples of inorganic adsorbents include natural zeolites, alumina, iron(III) hydroxide and diatomite.[12] Examples of organic adsorbents are coal and active carbon,[1] saw dust,[15] peat moss,[1] shellfish waste (chitin),[16,17] and biomass waste.[1,12,18] One of the most promising biopolymers for metal adsorption is *chitosan*, which is derived by deacetylation of chitin.[19] *Chitin* is a linear polysaccharide composed of randomly distributed β-(1,4)-linked D-

glucosamine (deacetylated unit) and *N*-acetyl-D-glucosamine (acetylated unit).[19-21] Chitin is the most widely occurring natural carbohydrate polymer, next to cellulose. This renewable compound is industrially prepared from shells of Crustacea (crabs, lobsters, shrimps, etc.) at low cost by removing other components, such as calcium and proteins, by treatment with acids and alkalis. The amine groups of chitosan are strongly reactive with metal ions.[22] These amine groups are thus responsible for the uptake of metal cations by a chelation mechanism.[23] The amine groups are easily protonated in acidic solutions and this may cause electrostatic attraction of anionic compounds, including metal anions (resulting from metal chelation by chloride, anionic ligands, etc.).[24,25] The chelation and ion-exchange mechanisms are in competition for the uptake of metal ions by chitosan. To avoid dissolution of chitosan in acidic aqueous solution, the material is chemically crosslinked with bi-functional reagents such as glutaraldehyde,[26] ethyleneglycol diglycidyl ether,[27] or hexamethylenediisocyanate.[28] Chitosan can easily be chemically modified by grafting metal coordinating groups to the amine or hydroxyl groups.[29] Examples include functionalization with EDTA, DTPA, 8-hydroxyquinoline or thiourea. This allows obtaining chitosan derivatives which are very selective for the uptake of given metals. For instance, DTPA- and EDTA-functionalized chitosan can be used for recovery of rare earths.[29-33] EDTA-functionalized chitosan also strongly binds calcium,[34] copper[33] or lead.[35] Chitosan functionalized with iminodiacetic acid (IDA) sequesters platinum and other platinum-group elements.[36] 8-Hydroxyquinoline-functionalized chitosan is selective for gallium,[37] and thiourea-functionalized chitosan is useful for sequestering of mercury,[38] and platinum-group elements.[39] An ascorbic chitosan derivative was studied for the uptake of uranium.[40] Besides the low cost and the readily availability from natural resources, a main advantage of functionalized chitosan is its high metal loading capacity. Modified chitosan can also be used as a stationary phase in liquid chromatography for the separation of mixtures of metal ions.[41,42] Inoue and coworkers have

studied the potential of a chromatographic column separation of rare earths with EDTA- and DTPA functionalized chitosan from sulfuric acid solutions.[29,32,33,43] The separation of samarium and yttrium was tested with EDTA-functionalized chitosan, whereas the separation of lanthanum, cerium, praseodymium and neodymium was investigated with a column packed with DTPA-functionalized chitosan. The author mentions as the main advantages of functionalized chitosan over synthetic cation exchange resins the lower price and the fact that no elution with solutions of chelating agents is required.

In this paper, the adsorption of rare earths from nitrate solutions with EDTA- and DTPA-functionalized chitosan was studied (Figure 1). In batch adsorption tests, different parameters were evaluated such as loading capacity, adsorption kinetics and influence of pH. A mixture of functionalized chitosan and silica was used as stationary phase for the separation of rare-earth ions in nitrate medium with medium pressure liquid chromatography (MPLC).

[Insert Figure 1 here]

Experimental

Materials and general methods

Ethylenediaminetetraacetic acid (99% pure) and diethylenetriaminepentaacetic acid (98+%) were purchased from Acros Organics. Acetic anhydride (Analytical Reagent) was purchased from Riedel-de Haën. Pyridine (AnalaR NORMAPUR®) was obtained from VWR. For the adsorption studies, highly viscous chitosan from crab shells with a deacetylation amount of approximately 80% was ordered from Fluka BioChemika. It consisted of white flake-shaped chitosan particles. For the chromatographic studies, lowly viscous chitosan from shrimp shells

was obtained from Sigma-Aldrich. It appeared as a powder. $Nd(NO_3)_3{\cdot}6H_2O$, $Pr(NO_3)_3{\cdot}6H_2O$, $Dy(NO_3)_3{\cdot}5H_2O$ and $Ho(NO_3)_3{\cdot}5H_2O$ (> 99.9%) were purchased from Sigma-Aldrich. Chelex® 100 was obtained from Bio-Rad Laboratories. All chemicals were used as received without further purification. EDTA bisanhydride and DTPA bisanhydride were synthesized according to a literature method described by Montembault *et al.* (see ESI).[44]

^1H and ^{13}C NMR spectra of organic intermediates were measured on a Bruker Avance 300 NMR spectrometer at 300 MHz for ^1H NMR and 75 MHz for ^{13}C NMR. FTIR spectra were measured on a Bruker Vertex 70 FTIR spectrometer with an ATR accessory (Platinum ATR). CHN (carbon, hydrogen, nitrogen) elemental analyses were obtained with the aid of a CE Instruments EA-1110 element analyzer. Luminescence spectra and decay curves were recorded on an Edinburgh Instruments FS900 spectrofluorimeter, equipped with a 450 W xenon arc lamp and 50 W microsecond flash lamp. Metal ion concentrations of the aqueous solutions after batch adsorption experiments were measured with Total Reflection X-ray Fluorescence (TXRF) on a Bruker S2 Picofox TXRF spectrometer. To perform the sample preparation for a TXRF measurement, an amount of the unknown metal ion aqueous solution (1–500 µL) is mixed in an eppendorf tube with a 1000 mg/L gallium standard solution (1–500 µL), diluted to 1 mL with demineralized water and stirred. It is important that the concentrations in the eppendorf tube are comparable for both the metal and the internal standard. A small amount of this prepared solution (about 10 µL) is put on a small quartz plate, pre-coated with a hydrophobic silicon solution, and dried in an oven at 60 °C. Optical absorption spectra were measured with a spectrophotometer Varian Cary 5000. Calibration curves for Pr^{3+}, Nd^{3+} and Dy^{3+} were prepared by making dilutions of 1000 ppm ICP-standard solutions of the corresponding elements. Since absorbance values were too low in the lower concentration regions with the standard 1 cm quartz cuvettes, quartz cuvettes with an optical path length of 10 cm were used.

Synthesis

EDTA-functionalized chitosan.

Chitosan (5 g, 31 mmol) was dissolved in a 10% (v/v) aqueous acetic acid solution (100 mL). The solution was diluted in methanol (400 mL). EDTA bisanhydride (23.83 g, 93 mmol), suspended in methanol (100 mL), was added to this solution and stirred for about 24 hours at room temperature to allow the reaction with the chitosan to proceed. After filtration, the precipitate was mixed with ethanol and stirred for another 12 hours. After filtering again, the precipitate was mixed with a 0.1 M NaOH solution (nearly 1L). More NaOH (in total equivalent to 0.2 M NaOH) had to be added gradually to the reaction mixture in order to effectively reach a pH of 11. This can be explained by the strong buffering effect of EDTA. It is however important not to bring functionalized chitosan into direct contact with the 0.2 M NaOH solution in order to avoid amide hydrolysis. The reaction mixture was stirred for another 12 hours. Non-reacted EDTA is converted to its sodium salt and thus dissolves in the aqueous phase. Next, the functionalized chitosan was filtered off. Because of the high viscosity of the reaction mixture, filtration was very slow. It was therefore important to find the right pore size of the sintered filter glass to achieve acceptable flow. The precipitate was washed several times with demineralized water, each time followed by centrifugation until the supernatant had a neutral pH. The precipitate was then mixed with a 0.1 M HCl solution and washed repeatedly with demineralized water until the pH of the washing water was neutral. After a stirring step in ethanol, followed by filtration, the product was dried in a vacuum oven at 40 °C for 48 hours to give a white solid. Yield: 36% (4.88 g; 11 mmol). IR (ATR, cm^{-1}, see ESI, Fig. S3): 3268 (broad band; O-H stretch + N-H stretch), 2875 (C-H stretch), 1725 (C=O stretch carboxylic acid), 1629 (C=O stretch amide), 1378 (symmetric vibration COO), 1032

(C-N stretch primary amine). For the degree of functionalization, the amount of nitrogen had to be considered before and after reaction. CHN elemental analysis for the original chitosan resulted in a nitrogen weight percentage of 7.25%, so that the amount of nitrogen in the original chitosan was calculated to be 11.68 g/mol. An analogous calculation for the functionalized chitosan material showed the nitrogen content to be 7.99% or 34.79 g/mol. Since one of three nitrogen atoms arise from the amide functionality in EDTA-chitosan, the degree of functionalization of the amine groups of chitosan is 99%. This value is very similar to literature results.[42]

DTPA-functionalized chitosan.

Chitosan (5 g, 31 mmol) was dissolved in a 10 % (v/v) aqueous acetic acid solution (100 mL). The solution was diluted in methanol (400 mL). DTPA bisanhydride (33.23 g, 93 mmol) was suspended in methanol (100 mL) and added to the chitosan solution. The crude product was purified in a similar way as described for EDTA-functionalized chitosan. Yield: 24% (3.92 g; 7.4 mmol). IR (ATR, cm^{-1}, see ESI, Fig. S4): 3250 (broad bend; O-H stretch + N-H stretch), 2878 (C-H stretch), 1726 (C=O stretch carboxylic acid), 1627 (C=O stretch amide), 1380 (symmetric vibration COO), 1033 (C-N stretch primary amine). The degree of functionalization of the amine groups of chitosan was calculated to be 94% on the basis of the nitrogen analysis results. This value is much higher than the value reported by Nagib et al. (22%).[42] This could be attributed to the larger excess of DTPA bisanhydride used for chitosan functionalization in the present paper. A second batch, making use of lowly viscous chitosan, gave a much higher yield: 49% (8.08 g; 15 mmol). The higher yield is a consequence of the fact that less washing steps were required for the lowly viscous chitosan. Moreover, filtration was much easier for lowly viscous chitosan, which facilitated the synthesis.

Adsorption experiments

Adsorption experiments were performed for three different lanthanide ions: the two neighboring light lanthanides neodymium (Nd^{3+}) and praseodymium (Pr^{3+}) and the heavy lanthanide dysprosium (Dy^{3+}). Concentrated stock solutions of these ions were made from the corresponding nitrate salts $Nd(NO_3)_3 \cdot 6H_2O$, $Pr(NO_3)_3 \cdot 6H_2O$ and $Dy(NO_3)_3 \cdot 5H_2O$ respectively. Proper dilutions of the stock solutions were prepared for the adsorption experiments. Each adsorption test was performed in 15 mL of aqueous metal ion solution. Functionalized chitosan (50 mg) was added to this solution that was then stirred with a magnetic stirring bar at a speed of 300 rpm at room temperature for a preset time period. The temperature is not increased in order to avoid hydrolysis of the formed amide functionality. After each adsorption experiment, the swollen chitosan loaded with adsorbed metal ions was separated from the aqueous solution with the aid of a 0.45 µm cellulose syringe filter.

Since it is rather difficult to measure the amount of metal adsorbed on the functionalized chitosan itself, the remaining metal ion concentration of the aqueous solution was determined. The amount of metal ions adsorbed onto the functionalized chitosan could then be determined with the following equation:

$$q = \frac{c_i - c_e}{m} . V \qquad (1)$$

Here q is the amount of adsorbed metal ions (mg/g adsorbent), c_i is the initial metal ion concentration in the aqueous solution (mg/L), c_e is the equilibrium metal ion concentration in

the aqueous solution, i.e. the concentration measured by TXRF after the adsorption experiment (mg/L), *V* is the volume of the solution (0.015 L) and *m* is the mass of the adsorbent (0.05 g). For the experimental conditions of the batch adsorption experiments, such as the duration of the adsorption, some optimization experiments were performed prior to the effective batch adsorption experiments. All optimization experiments were carried out with Nd^{3+}. Three parameters were investigated: (1) the influence of contact time, (2) the influence of metal ion concentration and (3) the influence of equilibrium pH of the aqueous solution.

By measuring the amount of adsorption as a function of the metal ion concentration at a certain temperature, a so-called *adsorption isotherm* is obtained. It can be observed that adsorption evolves to a certain plateau value. An adsorption isotherm thus provides information about the maximal loading capacity of an adsorbent at that specific pH and temperature. The adsorption isotherms could be fitted well with the Langmuir model. The *Langmuir adsorption model* is one of the most commonly used models for describing solute (metal ion) sorption to chitosan.[22,45-48] This model is based on the fact that a solid surface has a finite amount of sorption sites. It is further assumed that adsorption is a dynamical process. At equilibrium, the number of adsorbing ions equals the number of ions that are released by the adsorbent surface. The Langmuir equation is:

$$q = q_{max} \times \frac{K_{ads} . c_e}{1 + K_{ads} . c_e} \qquad (2)$$

In this equation, q is the amount of adsorbed metal ions (mg/g adsorbent), q_{max} is the maximal adsorption capacity of the adsorbent at that specific pH, K_{ads} is the adsorption equilibrium constant (L/mg) and c_e is the equilibrium metal ion concentration of the aqueous solution

(mg/L). By fitting the experimental data to this non-linear equation, values for the loading capacity of the chitosan and the adsorption equilibrium constant can be obtained.

Separation experiments

The potential of DTPA-chitosan for the chromatographic separation of rare-earth ions was tested and compared with the performance of the commercially available chelating cation exchange resin Chelex® 100 (Bio Rad Laboratories). This resin is a styrene-divinylbenzene copolymer containing iminodiacetic acid groups. Chromatographic separation experiments were carried out by medium pressure liquid chromatography (MPLC). The setup was composed of a Büchi chromatography pump B-688 to control the pressure and the eluent delivery flow and a glass Büchi BOROSILIKAT 3.3 column tube, N° 17988 with dimensions 9.6 mm × 115 mm (bed volume = 8.3 mL). The stationary phase was a mixture of DTPA-chitosan and silica in a 1:5 mass ratio. It has been observed by other authors that chitosan-silica hybrid materials have better mechanical properties than pure chitosan.[49,50] We found that without the use of silica, no smooth liquid flow through the column could be obtained. In addition, highly viscous chitosan has to be avoided. DTPA-chitosan was prepared starting from lowly viscous chitosan from shrimp shells. The MPLC column was packed with a slurry, made by homogeneously mixing 1 g of chitosan gel, swollen in an aqueous HNO_3 solution at pH 3, with 5 g of silica gel 60 (particle size between 0.015 and 0.040 mm). Flow rates up to 20 mL/min could be reached without exceeding the maximum pressure, which was set at 10 bar. Each experiment was preceded by a thorough washing of the column with 50 mL of demineralized water, followed by conditioning of the column with 25 mL of an acetate buffer at pH 3. After each experiment, the column was stripped with 50 mL of an aqueous 1M HNO_3 solution, followed by washing with 50 mL of demineralized water. In order to avoid

degradation, the Chelex® 100 resin had to be reconverted to the sodium form after each experiment by rinsing the column with 50 mL of an aqueous 1M NaOH solution. Separated compounds were collected with the aid of a Büchi Automatic Fraction Collector B-684. Fraction collection was monitored by *ex-situ* analysis of the fractions by UV/VIS spectroscopy to determine the respective metal ion concentrations. This method was selected because it is much faster than TXRF as no time-consuming sample preparation is required. The separation experiments were done with Pr^{3+}, Nd^{3+} and Ho^{3+}. The original focus of this work was on separations relevant to magnetic recycling (NdFeB magnets), so that praseodymium, neodymium and dysprosium are the most relevant elements for a separation study. However, although Pr^{3+} and Nd^{3+} show both intense absorption bands in the visible region of the electromagnetic spectrum, the absorption bands of Dy^{3+} were too weak to be useful for concentration determination by UV/VIS spectroscopy. Therefore, it was decided to use holmium (Ho^{3+}) instead. Holmium is the lanthanide element following dysprosium in the periodic table and it has strong absorption bands in the visible region. The difference in ionic radius between Dy^{3+} and Ho^{3+} is very small so that no significantly different complex formation behavior is expected. Based on the absorbance spectra, appropriate wavelength values for analysis were chosen, being 444.0 nm for Pr^{3+}, 740.5 nm for Nd^{3+} and 536.5 nm for Ho^{3+} (see ESI, Fig. S1). For Pr^{3+}, it was hard to find an appropriate wavelength since each peak overlaps with a peak of either Nd^{3+} or Ho^{3+}. An interference test confirmed that, at 444.0 nm, the tail of the Ho^{3+} absorption peak can be assumed to be negligible. A calibration curve could be made for the respective wavelengths by analyzing aqueous solutions of different concentrations, ranging from 10 to 1000 ppm (see ESI, Fig. S2).

Results and Discussion

Synthesis of chitosan derivatives and characterization of lanthanide complexes

Chitosan was functionalized with EDTA and DTPA by reaction with the corresponding bisanhydrides.[42] The binding of lanthanide ions to EDTA- or DTPA-functionalized chitosan can be observed by measuring FTIR spectra. This was done for the adsorption of Nd^{3+} ions. In the absence of chelate rings the wavenumber of the C-H absorption peak is 2875 cm^{-1}. The shift to a higher wavenumber (to 2945 cm^{-1}) by chelating Nd^{3+}, suggests that the metal ion has an effect on the vibration of the C-H bond and must be attached to the COO^- groups of the EDTA/DTPA functional groups.[51] The shift to the highest possible wavenumbers for the C-H stretch (approaching 3000 cm^{-1}) suggests that the chelating complex is rather strong. Further, the presence of absorption bands at 1582 cm^{-1} and 1379 cm^{-1}, arising from the asymmetric and the symmetric vibration of carboxylate, respectively, can be observed in the Nd(III)-chelated chitosan spectra, whereas these absorption bands were not observable before complex formation with Nd(III). Hence, these species contain COOH groups instead. Moreover, the observation of the asymmetric carboxylate vibration at a wavenumber lower than 1610 cm^{-1} indicates that the metal ion is bonded electrostatically to the carboxylate groups of EDTA and DTPA. Finally, the disappearance of N-H bend of the amide was observed in the spectra of the metal-chelated chitosans, probably due to conformational reasons. After having performed an adsorption experiment with EDTA-chitosan in an aqueous solution containing Eu^{3+}, it was possible to record a luminescence spectrum of the europium(III)-EDTA-chitosan complex (Figure 2). The pattern, shape and relative intensities of the peaks can provide information about the environment of the Eu^{3+} ion. Since the excitation spectrum was dominated by a peak at 395 nm (corresponding to the $^7F_0 \rightarrow {}^5L_6$

transition), the emission spectrum was recorded by irradiation of the sample at this wavelength. The transitions in the luminescence spectrum originate from the $^5D_0$ level and terminate at the various ^7F_J levels (J = 0 – 4): $^5D_0 \rightarrow {}^7F_0$ at 580 nm, $^5D_0 \rightarrow {}^7F_1$ at 595 nm, $^5D_0 \rightarrow {}^7F_2$ at 615 nm, $^5D_0 \rightarrow {}^7F_3$ at 650 nm and $^5D_0 \rightarrow {}^7F_4$ at 700 nm. The $^5D_0 \rightarrow {}^7F_2$ hypersensitive transition is the most intense transition in the europium–coordinated EDTA-chitosan complex. The presence of the $^5D_0 \rightarrow {}^7F_0$ transition indicates that the point group symmetry of the Eu^{3+} site is C_n, C_{nv} or C_s.[52] The fact that this transition appears as a single peak in the luminescence spectrum indicates that the Eu^{3+} ions occupy no more than one site of symmetries C_n, C_{nv} or C_s. Unfortunately, the crystal-field fine structure was not sufficiently resolved to assign the exact symmetry of the Eu^{3+} site.

[Insert Figure 2 here]

The hydration number q of Eu^{3+} ion in europium(III)-coordinated functionalized chitosan complexes was determined by recording the decay time of the $^5D_0$ excited state (measured by monitoring the luminescence intensity of the hypersensitive $^5D_0 \rightarrow {}^7F_2$ transition at 613.50 nm) for the europium(III)-coordinated functionalized chitosan complexes suspended in H_2O and D_2O, and by applying the Horrocks-Supkowski equation:[53]

$$q = 1.11 \times \left(\frac{1}{\tau_{H2O}} - \frac{1}{\tau_{D2O}} - 0.31\right) \quad (3)$$

The hydration number *q* is the number of water molecules in the first coordination sphere of the Eu^{3+} ion. τ_{H2O} and τ_{D2O} are the luminescence decay times measured in water and heavy water, respectively. The Horrocks-Supkowski formula is a modification of the original Horrocks-Sudnick equation.[54] From three independent measurements, an average lifetime value was calculated. For EDTA-chitosan, the average lifetime of the coordinated europium(III) was 0.671 ms in D_2O, whereas it was 0.186 ms in H_2O. For DTPA-chitosan, the average lifetime of the coordinated europium(III) was 1.502 ms in D_2O, whereas it was 0.518 ms in H_2O. The hydration number for the adsorbed Eu^{3+} ion was therefore calculated from equation (3) to be 3.98 (rounded to 4) for EDTA-chitosan, respectively 1.06 (rounded to 1) for DTPA-chitosan. Assuming that europium(III) coordinates with five atoms of the EDTA-moiety (two nitrogen atoms and three oxygen atoms), four water molecules lead to a coordination number of nine. In DTPA-chitosan, seven atoms are available for coordination (three nitrogen atoms and four oxygen atoms). With one additional water molecule coordinated, europium(III) would be 8-coordinated in DTPA-chitosan.

Batch adsorption studies

Batch adsorption experiments were first carried out with aqueous solutions of $Nd(NO_3)_3$ to find the optimized adsorption parameters. The influence of the contact time on the adsorption amount was investigated for both EDTA- and DTPA-chitosan. The experiment was carried out twice with a chosen metal ion concentration of 200 ppm and no pH adjustments were made. The adsorption equilibrium conditions were reached for both EDTA-chitosan and DTPA-chitosan after about 4 hours of stirring (Figure 3). As a consequence of this observation it was decided to perform all further adsorption experiments for 4 hours. Adsorption equilibrium seems to be reached faster for EDTA-chitosan in comparison with

DTPA-chitosan. This observation is attributed to the smaller particle size of EDTA-chitosan (more like a powder) than that of DTPA-chitosan (more grain-like particles), which promotes faster swelling of the chitosan particles. However, the loading capacity (plateau value) is comparable for both materials. Since it is expected that the immobilized functional groups are mainly responsible for the complexation of metal ions, the adsorption amount is suggested to be a merely thermodynamic aspect of the adsorption process. It is therefore hypothesized that differences in particle size will not have significant consequences for later adsorption experiments in which affinity and selectivity differences will be investigated (thermodynamics versus kinetics).

[Insert Figure 3 here]

The influence of the equilibrium metal ion concentration in solution on the metal ion adsorption amount was investigated for EDTA- and DTPA-chitosan and compared with non-modified chitosan (Figure 4). No pH adjustments were made. The total amount of Nd^{3+} adsorbed by the original, non-functionalized chitosan is very small (< 10 mg Nd^{3+}/g chitosan). The adsorption capacities of EDTA- and DTPA-chitosan are very similar. Langmuir fitting gives a maximum loading capacity of 74 mg/g for EDTA-chitosan and 77 mg/g for DTPA-chitosan. However, the adsorption equilibrium constant *K* (obtained from Langmuir modeling) for DTPA-chitosan (0.19) is larger than that of EDTA-chitosan (0.04). In analogy, the stability constant of Nd^{3+} with DTPA (21.6) is larger than with EDTA (16.6).[55] The graph thus confirmed the assumption that DTPA-chitosan is a stronger complex former for Nd^{3+} than EDTA-chitosan.

[Insert Figure 4 here]

The influence of equilibrium pH on the adsorption amount was investigated for EDTA-chitosan and DTPA-chitosan. The experiment was performed with a metal ion concentration of 300 ppm. Adjustments of the pH were made with a concentrated HNO_3 solution for lowering the pH and a concentrated NaOH solution for raising the pH. The equilibrium pH of the metal ion solution was approximately 3 when no pH adjustments were made, while the pH of the *initial* feed solution was approximately 6. This lowering of the aqueous pH during the adsorption experiment is attributed to ion exchange with chitosan. Carboxyl protons on chitosan are exchanged for trivalent rare-earth ions in solution, thus lowering the pH. The observation that adsorption already occurs from a pH of 1 is quite surprising (Figure 5). Based on the speciation curves of aqueous EDTA and DTPA, their carboxyl groups are still protonated at this pH (pK_{a3}(EDTA) = 2.0).[56] Also, the optimum adsorption value is reached at a pH of 3-4, where EDTA and DTPA are not expected to be fully deprotonated (pK_{a5}(EDTA) = 6.1).[56] These observations can be partly explained by the absorption effect of chitosan besides the ion exchange process. Some lanthanide ions are probably caught in the dense chitosan network without being complexated by the functional ligands on it. However, it should also be noted that the chelating ability of immobilized EDTA and DTPA functional groups at low pH values has been observed elsewhere. This can be assigned to inductive effects that decrease pK_a values of immobilized EDTA/DTPA-carboxylate groups.[57] Although it can be observed that maximal adsorption occurs for pH > 4 for both EDTA- and DTPA-chitosan, the interesting pH region is situated in the lower pH region, at pH 1–3. In this pH region, differences in adsorption capacity exist for different pH values. Also affinity differences between distinct lanthanide ions can thus be predicted in this

pH region. With the eventual separation of rare earths in mind, all following adsorption experiments, focused therefore on the lower pH region (pH = 1 to 2).

[Insert Figure 5 here]

It was investigated whether differences exist in the amount of different lanthanide ions adsorbed as a function of the equilibrium pH of the metal ion solution (pH 1–2). This is illustrated in Figure 6 for DTPA-chitosan, for the lanthanides Pr^{3+}, Nd^{3+} and Dy^{3+}. In this figure, the distribution coefficient is plotted as a function of the equilibrium pH of the aqueous solution. In the context of adsorption processes, a distribution coefficient *D* is defined as:

$$D = 1000\ \frac{mL}{L} \times \frac{q}{c_e} \qquad (4)$$

Here q is the amount of solute (metal ions) adsorbed onto the adsorbent (functionalized chitosan) (mg/g) and c_e is the equilibrium metal ion concentration in solution (mg/L). Figure 6 shows that the three lanthanides are effectively adsorbed on DTPA-chitosan, even at very low pH values. The order of affinity among the metal ions is: $Dy^{3+} > Nd^{3+} > Pr^{3+}$. However, this difference in affinity is only pronounced in the region where the chitosan loading is relatively low. At pH > 2, no affinity differences can be observed. The limiting behavior in the low pH region can be attributed to the competition between protons and metal ions for the available sorption sites. By analogy with the experiments performed by Inoue and coworkers,[29] a linear

fit with a fixed slope of three was plotted for the three elements. Being the valence state of the rare-earth ions, a slope of three indicates the exchange of three EDTA-chitosan protons for one trivalent metal ion (notice the logarithmic scale of the Y-axis, since also the pH is logarithmically correlated with the H_3O^+ concentration). The results for EDTA-chitosan are very comparable with the results obtained for DTPA-chitosan (see ESI, Fig. S5).

[Insert Figure 6 here]

Since the separation of Nd^{3+} and Dy^{3+} is industrially relevant for the recycling of rare earths from end-of-life permanent magnets (as Nd and Dy are both present in neodymium-iron-boron magnets),[58] the batchwise adsorption of these two elements was further investigated in binary solutions as this is a better way to investigate the effective selectivity for both elements due to the competition that occurs between both metal ions. A binary solution of Nd^{3+} and Dy^{3+} with a molar 1:1 ratio of Nd^{3+} to Dy^{3+} was prepared. The influence of the equilibrium pH on the selective adsorption amount was investigated for EDTA-chitosan and DTPA-chitosan. In Figure 7, the more selective adsorption of Dy^{3+} in comparison with Nd^{3+} is presented for DTPA-chitosan as a function of the equilibrium pH of the aqueous solution, containing 0.693 mmol Nd^{3+} and 0.708 mmol Dy^{3+}. A higher adsorption amount (and thus selectivity) is observable for Dy^{3+} in comparison with Nd^{3+}. It also becomes clear from Figure 7 that this difference in selectivity increases by lowering the pH. At pH = 1, Nd^{3+} is barely adsorbed. Contrarily, a significant amount of Dy^{3+} stays complexed to the functionalized chitosan at this low pH value. This observation is consistent with previous observations in one-component systems. Analogous observations resulted from the experiments with EDTA-chitosan (see ESI, Fig. S2). The adsorption results from these

experiments were used to calculate enrichment factors of Dy^{3+} in comparison with Nd^{3+} as a function of equilibrium pH. Enrichment factors quantify the higher adsorption of Dy^{3+} in comparison with Nd^{3+} by taking the ratio of the portion of Dy^{3+} on the chitosan to the portion of Dy^{3+} in the initial solution. An enrichment factor of 3 thus means that the portion of Dy^{3+} (compared to Nd^{3+}) onto the adsorbent surface is three times higher than in the initial solution. The results are depicted in Figure 8. An enrichment factor of 1 actually means that no enrichment occurs. Since there is no selectivity at the respective pH, equal amounts of Nd^{3+} and Dy^{3+} are adsorbed. However, it is evident from Figure 8 that enrichment in Dy^{3+} increases with decreasing pH values. Furthermore, Figure 8 shows that DTPA-chitosan gives better separations of Nd^{3+} and Dy^{3+}: enrichment factors up to 4 can be reached with DTPA-chitosan, compared to a value of 2.5 with EDTA-chitosan.

[Insert Figures 7 and 8 here]

Experiments have been carried out to investigate the reusability of the functionalized chitosan materials after stripping of the adsorbed metal ions. Nd^{3+} was first adsorbed from a $Nd(NO_3)_3$ stock solution having a Nd concentration of 985 ppm. To desorb the metal from the adsorbent surface after an adsorption experiment, the used chitosan was shortly stripped with 2M HNO_3. After filtering the chitosan and washing it several times with demineralized water, the swollen chitosan was dried in the vacuum oven at 40 °C until a constant weight was achieved. Then it could be reused in another adsorption experiment. The whole procedure was repeated three times, resulting each time in an adsorption amount that was comparable with the adsorption amount of DTPA-chitosan when used for the first time. It was observed that each stripping step lowers the efficiency of the chitosan by about 2% (See ESI, Table S1). A

possible explanation for this observation is damage occurs (like amide hydrolysis) by treating the chitosan with highly concentrated acid during the stripping step. Notice that non-functionalized chitosan dissolves in an acidic environment. The loss in efficiency for metal ion adsorption after regeneration can probably be minimized by stripping with less concentrated acid solutions. It is suggested that 1M HCl should be acidic enough.

Chromatographic separation of rare earths

The first separation experiments were carried out on Nd^{3+}/Ho^{3+} mixtures. The solutions were made from the corresponding nitrate salts. For the first aqueous solution, concentrations of Nd^{3+} and Ho^{3+} were analyzed by UV/VIS spectroscopy to be 1240 ppm and 1250 ppm, respectively (ratio 1:1 wt/wt). The pH of the aqueous solution was adjusted to a value of 3. A first experiment was carried out with the commercially available Chelex® 100 resin. A sample solution (5 mL) was introduced on the top of the chromatography column after conditioning of the column to a pH of 3. Next, the column was eluted with 200 mL of an aqueous HNO_3 solution at pH 3. Since no migration of metal ions was observed at this pH, pH was lowered gradually. First, 200 mL of an aqueous HNO_3 solution at pH 2.75 was pumped through the column, followed by 200 mL of pH 2.50, 200 mL of pH 2.25 and eventually 1000 mL of pH 2 as migration of the ions through the column only started at this pH. At higher pH values, the lanthanide ions seemed to be bound too strongly to the Chelex® 100 resin. The flow rate was 6.2 mL/min. Fractions of 20 mL were collected. The resulting chromatogram is shown in the ESI (Fig. S7). No actual separation of Nd^{3+} and Ho^{3+} was observed on the chromatogram with Chelex® 100. Although Nd^{3+} eluted from the column with a small time delay, the two peaks can be largely considered to be overlapping. This observation is not surprising. At a pH of 2, Chelex® 100 is no longer functional, due to the

positive charge of the resin at this pH. However, the low pH was needed to break the strong interactions between the resin and the lanthanide ions, inhibiting their movement. Given the strong affinity of Chelex® 100 for rare-earth ions, it can be concluded that this system could be useful to separate them from other elements, but not to mutually separate them from each other under these experimental conditions. It was not tried to improve the separation with Chelex® 100 by eluting the column with a solution of a complexing agent (such as EDTA, citric acid or α-hydroxy isobutyric acid). The column separation experiment was repeated with the resin containing a mixture of DTPA-chitosan (lowly viscous) and silica, homogeneously mixed in a 5:1 mass ratio. Again 5 mL of the Nd^{3+}/Ho^{3+} sample solution was added on the top of the column after conditioning the column to a pH of 3. Making use of the knowledge gained from the batch adsorption experiments, it was decided to immediately elute the lanthanide ions with an aqueous HNO_3 solution at pH 1. The resulting flow rate of 2 mL/min was lower compared to the Chelex® 100 system because of the higher viscosity of the chitosan-silica packing. Fractions of 10 mL were collected. A distinct improvement with respect to Chelex® 100 was observed. The peaks of Nd^{3+} and Ho^{3+} are no longer lying on top of each other (see Figure 9). Partial overlap of the peaks can still be observed although large part of the fractions is completely pure in Nd^{3+} while these ions become negligibly present in the last Ho^{3+} fractions. An attempt was made to optimize the separation further. Therefore, the experiment was repeated with a lower flow rate (1 mL/min) and a different eluent pH. As the stripping effect is significant at pH 1, it was decided to increase the pH of the aqueous HNO_3 solution to 1.25. At this pH it was observed that initially only Nd^{3+} 'broke through' as is visualized in the breakthrough curve (Figure 10). After a while, also low amounts of Ho^{3+} started to elute, but only small amounts and not in a usual bell-shaped elution band. Next, the column was stripped with an aqueous 1M HNO_3 solution (pH 0). In fact, this is done after each experiment, but this time, the resulting fractions were also collected and analyzed by

UV/VIS spectroscopy. In the elution curve (see ESI, Fig. S8), all remaining Ho^{3+} was collected from the column in a few fractions, with negligible contamination of remaining Nd^{3+} ions.

Also the effect of a Nd^{3+} excess on the separation performance of the chitosan column was investigated. In NdFeB-magnets for example, Nd^{3+} is present in large excess with respect to Dy^{3+}.[58] An aqueous solution with a mixture of Nd^{3+}/Ho^{3+} was made with a Nd^{3+} concentration of 5410 ppm and a Ho^{3+} concentration of 555 ppm; thus the ratio is considered to be about 10:1 wt/wt. The pH of the solution was adjusted to a value of 3. As in the experiment with the 1:1 ratio, 5 mL of the sample solution was added on the top of the chromatography column after conditioning the column to a pH of 3. The column was eluted with 200 mL of an aqueous HNO_3 solution at pH 1.25. The flow rate was again 1 mL/min. Fractions of 10 mL were collected. Despite changing the composition of the sample, the same trend as before was observed: Nd^{3+} completely eluted from the column at a breakthrough pH of 1.25 (see ESI, Fig. S9). When all Nd^{3+} was considered to be collected, an elution curve of Ho^{3+} resulted by stripping the column with an aqueous 1M HNO_3 solution. Despite being present in much smaller amounts than Nd^{3+}, the Ho^{3+} stripping fractions contained only traces of Nd^{3+}. In practice, all fractions collected after the breakthrough of Nd^{3+} could be subjected to another separation cycle to get more pure Nd^{3+} and Ho^{3+}. By further optimizations, an efficient separation method for the two elements could be developed on an industrial scale.

[Insert Figures 9 and 10 here]

The neighboring elements praseodymium and neodymium are very difficult to separate. However, since both elements are found in NdFeB magnet mixtures, their separation

is relevant. Given the challenge of the Pr^{3+}/Nd^{3+} separation, the resulting chromatogram can be seen as a worst case scenario for the separating ability of the DTPA-chitosan/silica resin. An aqueous solution containing a mixture of Pr^{3+} and Nd^{3+} was made, starting from the corresponding nitrate salts. The concentrations of Pr^{3+} and Nd^{3+} were measured to be 1060 ppm and 1020 ppm, respectively. The resulting ratio of the binary solution is thus considered to be 1:1. The pH of the solution was adjusted to a value of 3. 5 mL of the sample solution was introduced to the top of the chromatographic column after conditioning the column to a pH of 3. To find the breakthrough pH, the column was eluted consecutively with 50 mL of an aqueous HNO_3 solution at pH 1.50, 1.45, 1.40, 1.35, 1.30 and 1.25. The flow rate valued 0.75 mL/min. Fractions of 10 mL were collected. Since Pr^{3+} and Nd^{3+} are so similar in chemical properties, it was not possible to distinct the breakthrough of Pr^{3+} and elution of Nd^{3+}. Nevertheless, the resulting separation of the peaks in the chromatogram is quite reasonable, taking into account the difficulty of this separation (see ESI, Fig. S10). The two peaks overlap partially, but are clearly separated from each other. The DTPA-chitosan/silica chromatography column shows a higher selectivity for Nd^{3+} compared to Pr^{3+}.

The column separation performance was ultimately investigated by subjecting the DTPA-chitosan/silica column to a ternary mixture of the ions Pr^{3+}, Nd^{3+} and Ho^{3+}. An aqueous solution of $Pr^{3+}/Nd^{3+}/Ho^{3+}$ was prepared starting from the corresponding nitrate salts. The concentrations were measured to be 490 ppm for Pr^{3+}, 510 ppm for Nd^{3+} and 490 ppm for Ho^{3+}; thus, the ratio of the resulting solution is considered to be 1:1:1 on a mass basis. 5 mL of the sample solution was brought on the top of the column after conditioning of the column. With the knowledge of previously derived breakthrough pH values, it was decided to elute the column consecutively with 50 mL of an aqueous HNO_3 solution at pH 1.50 (breakthrough of Pr^{3+}), pH 1.25 (breakthrough of Nd^{3+}) and pH 1.00 (breakthrough of Ho^{3+}), followed by stripping with 1M HNO_3. The flow rate was 1.25 mL/min. Fractions of 10 mL were collected.

The chromatogram is presented in Figure 11. The three elements are not completely separated from each other, though at least an important enrichment occurs by applying this ion-exchange method with functionalized chitosan to the mixed metal-ion solution. The chromatogram clearly shows that the elements Pr and Ho could be separated from each other in a first cycle, with both fractions still containing a lot of Nd. In a second cycle, both fractions could be subjected on their turn to a separation cycle in order to mutually separate Pr/Nd and Nd/Ho, respectively.

[Insert Figure 11 here]

Besides the promising separation results obtained with DTPA-chitosan, several other advantages of using functionalized chitosan instead of Chelex® 100 became evident during the separation experiments. A first advantage is related to the swelling behavior in aqueous solutions. Whereas it is well known of chitosan to swell significantly by going from a powder to a gel by soaking it with water, the amount of swelling did not seem to be dependent on the ions present in the aqueous solution. The volume of the chitosan packing in the column did thus not change by changes in the pH of the eluent. The volume of Chelex® 100 on the other hand was strongly dependent on the type (size) of ions bound to the resin. By going from the sodium form to the lanthanide form, the Chelex® 100 cation exchanger significantly increased in volume. By decreasing the pH, nothing happened at first instance, because the lanthanide ions were bound too strongly to the resin, until the point that the resin functional groups became positively charged by protonation. The exchange of large lanthanide ions for small protons caused a dramatic volume decrease of the resin. This collapse of the resin probably explains partly the poor separation that was observed for Chelex® 100. Another advantage of

DTPA-chitosan is the faster separation rate by DTPA-chitosan. This is probably due to the fact that by a proper packing with silica, places of rapid ion exchange with chitosan are well combined with open pathways for the ions to move through the column along the silica. With the right pH conditions, the sample ions immediately start to migrate down the column with a retention that is dependent on the type of ion. With Chelex® 100, it took a much longer time before the ions were eluted from the column despite the higher flow rates that were used. The assumption is made that this again can be attributed to the swelling behavior of Chelex® 100. The local swelling of the resin with the downwards movement of large lanthanide ions through the resin could prevent a smooth passage of the ions through the column. It has to be mentioned also that Chelex® 100 degrades when it is not in the sodium form. After each experiment, the column with a packing of Chelex® 100 had to be rinsed with a NaOH solution, whereas the performance of chitosan is not influenced by the form in which it is stored, either it is in a wet, a dry, an acidic or an alkaline environment. Another advantage of DTPA-chitosan is the effective reusability of the DTPA-chitosan/silica packing. The adsorption/desorption behavior of DTPA-chitosan did not change during consecutive experiments. A final advantage is that a good separation of rare-earth ions is possible by simply eluting with a simple dilute acid solution like nitric acid, whereas the separation of rare-earth ions with cation exchange columns requires elution with solutions of chelating agents such as EDTA, citric acid or α-hydroxy isobutyric acid.[59,60]

Conclusions

Chitosan was modified with EDTA and DTPA groups and the resulting material was used for the adsorption of trivalent rare-earth ions from acidic nitrate solutions. The performance of the modified chitosan was tested for batch adsorption tests with

neodymium(III). Different parameters such as loading capacity, adsorption kinetics and pH of the aqueous feed solution were tested. It was shown that adjustment of the pH could be used to achieve selectivity in adsorption of different rare-earth ions by adjustment of the pH of the aqueous solution. The modified chitosans were used as a stationary phase for chromatographic separations of rare-earth ions by medium pressure liquid chromatography (MPLC). It was shown that the type of chitosan (with a high or low viscosity) is an important parameter for designing efficient chromatographic separation procedures with functionalized chitosan packed into a column, because the flow rates of the eluent can be much too low to be of practical use with highly viscous chitosan. The best type of stationary phase was obtained by using the functionalized chitosan (made of chitosan with a low viscosity) in a more rigid matrix of silica gel. It was shown that the functionalized chitosan could be used for separation of mixtures of rare-earth ions with a dilute nitric acid solution as eluent, without the need of chelating agents. The separation was investigated for Nd^{3+}/Ho^{3+}, Pr^{3+}/ Nd^{3+} and $Pr^{3+}/ Nd^{3+}/Ho^{3+}$ mixtures. The results show that upon optimization of the chromatographic procedure and upscaling, separation of mixtures of rare earths with columns filled with EDTA- or DTPA-functionalized chitosan would be feasible.

Acknowledgments

The authors thank the KU Leuven for financial support (research project GOA 13/008 and IOF-KP RARE^3). Neil R. Brooks and Brecht Egle are acknowledged for useful discussions and suggestions about the experimental work. CHN analyses were carried out by Dirk Henot.

Electronic supporting information

Electronic supplementary information (ESI) available: optical absorption spectra of aqueous solutions (1000 ppm) of Pr^{3+}, Nd^{3+} and Ho^{3+}; calibration curves for Pr^{3+} (444.0 nm), Nd^{3+} (740.5 nm) and Ho^{3+} (536.5 nm); synthesis of EDTA bisanhydride and DTPA bisanhydride; IR spectra of EDTA-chitosan and DTPA-chitosan; figures with additional curves of adsorption experiments and chromatographic separation; table with efficiency values of DTPA-chitosan for Nd^{3+} adsorption after consecutive regenerations (reuse of DTPA-chitosan).

References

1 S. E. Bailey, T. J. Olin, R. M. Bricka and D. D. Adrian, *Water Res.*, 1999, **33**, 2469-2479.

2 F. L. Fu and Q. Wang, *J. Environ. Manage.*, 2011, **92**, 407-418.

3 C. Mack, B. Wilhelmi, J. R. Duncan and J. E. Burgess, *Biotechnol. Adv.*, 2007, **25**, 264-271.

4 S. De Corte, T. Hennebel, B. De Gusseme, W. Verstraete and N. Boon, *Microb. Biotechnol.*, 2012, **5**, 5-17.

5 T. Hennebel, B. De Gusseme, N. Boon and W. Verstraete, *Trends Biotechnol.*, 2009, **27**, 90-98.

6 M. G. Roig, T. Manzano and M. Diaz, *Water Res.*, 1997, **31**, 2073-2083.

7 F. Haber, *Angew. Chem.*, 1927, **40**, 303-314.

8 R. A. A. Muzzarelli, *Carbohyd. Polym.*, 2011, **84**, 54-63.

9 T. Kakoi and M. Goto, *Nippon Kaisui Gakkaishi*, 1997, **51**, 319-324.

10 R. A. Beauvais and S. D. Alexandratos, *React. Funct. Polym.*, 1998, **36**, 113-123.

11 H. Matsunaga, *Bunseki Kagaku*, 2001, **50**, 89-106.

12 S. Babel and T. A. Kurniawan, *J. Hazard. Mater.*, 2003, **97**, 219-243.

13 G. Crini, *Prog. Polym. Sci.*, 2005, **30**, 38-70.

14 M. Minamisawa, H. Minamisawa, S. Yoshida and N. Takai, *J. Agr. Food Chem.*, 2004, **52**, 5606-5611.

15 Y. F. Zhou and R. J. Haynes, *Crit. Rev. Env. Sci. Tec.*, 2010, **40**, 909-977.

16 J. K. Dutkiewicz, *J. Biomed. Mater. Res.*, 2002, **63**, 373-381.

17 Coughlin, R. W. Partially treated shellfish waste for removal of heavy metals from aqueous solution. US5010181A, Apr 23, 1991.

18 D. Sud, G. Mahajan and M. P. Kaur, *Bioresource Technol.*, 2008, **99**, 6017-6027.

19 M. N. V. R. Kumar, *React. Funct. Polym.*, 2000, **46**, 1-27.

20 M. Rinaudo, *Prog. Polym. Sci.*, 2006, **31**, 603-632.

21 N. K. Mathur and C. K. Narang, *J. Chem. Educ.*, 1990, **67**, 938-942.

22 F. C. Wu, R. L. Tseng and R. S. Juang, *J. Environ. Manage.*, 2010, **91**, 798-806.

23 A. J. Varma, S. V. Deshpande and J. F. Kennedy, *Carbohyd. Polym.*, 2004, **55**, 77-93.

24 E. Guibal, *Sep. Purif. Technol.*, 2004, **38**, 43-74.

25 P. Chassary, T. Vincent and E. Guibal, *React. Funct. Polym.*, 2004, **60**, 137-149.

26 O. A. C. Monteiro and C. Airoldi, *Int. J. Biol. Macromol.*, 1999, **26**, 119-128.

27 A. Neira-Carrillo, J. Retuert, F. Martinez and J. L. Arias, *J. Chil. Chem. Soc.*, 2008, **53**, 1367-1372.

28 A. D. Gonsalves, C. R. M. Araujo, N. A. Soares, M. O. F. Goulart and F. C. de Abreu, *Quim. Nova*, 2011, **34**, 1215-1223.

29 K. Inoue and Y. Baba, Chitosan: A versatile biopolymer for separation, purification, and concentration of metal ions. In *Ion Exchange and Solvent Extraction, Vol. 18*, ed. A. K. Sengupta, CRC Press, Boca Raton, 2007, pp 339-374.

30 V. Darras, M. Nelea, F. M. Winnik and M. D. Buschmann, *Carbohyd. Polym.*, 2010, **80**, 1137-1146.

31 K. Inoue, K. Ohto, K. Yoshizuka, R. Shinbaru, Y. Baba and K. Kina, *Bunseki Kagaku*, 1993, **42**, 725-731.

32 K. Inoue, Chromatographic separation of rare earths with complexane types of chemically modified chitosan. In *Advances in Chitin Science Vol 4. (Proceedings of the 3rd International Conference of the European Chitin Society)*, ed. M. G. Peter, A. Domard and R. A. A. Muzzarelli, Universität Potsdam, Potsdam, 2000, pp 460-465.

33 K. Inoue, K. Ohto, K. Yoshizuka, R. Shinbaru and K. Kina, *Bunseki Kagaku*, 1995, **44**, 283-287.

34 Y. Shimizu, S. Izumi, Y. Saito and H. Yamaoka, *J. Appl. Polym. Sci.*, 2004, **92**, 2758-2764.

35 K. Inoue, K. Ohto, K. Yoshizuka, T. Yamaguchi and T. Tanaka, *Bull. Chem. Soc. Jpn.*, 1997, **70**, 2443-2447.

36 K. Inoue, T. Yamaguchi, M. Iwasaki, K. Ohto and K. Yoshizuka, *Sep. Sci. Technol.*, 1995, **30**, 2477-2489.

37 K. Inoue, H. Hirakawa, Y. Ishikawa, T. Yamaguchi, J. Nagata, K. Ohto and K. Yoshizuka, *Sep. Sci. Technol.*, 1996, **31**, 2273-2285.

38 K. C. Gavilan, A. V. Pestov, H. M. Garcia, Y. Yatluk, J. Roussy and E. Guibal, *J. Hazard. Mater.*, 2009, **165**, 415-426.

39 A. Butewicz, K. C. Gavilan, A. V. Pestov, Y. Yatluk, A. W. Trochimczuk and E. Guibal, *J. Appl. Polym. Sci.*, 2010, **116**, 3318-3330.

40 I. Saucedo, E. Guibal, C. Roulph and P. Lecloirec, *Environ. Technol.*, 1992, **13**, 1101-1115.

41 K. Inoue, K. Yoshizuka and K. Ohto, *Anal. Chim. Acta*, 1999, **388**, 209-218.

42 S. Nagib, K. Inoue, T. Yamaguchi and T. Tamaru, *Hydrometallurgy*, 1999, **51**, 73-85.

43 K. Inoue and S. Alam, *JOM*, 2013, **65**, 1341-1347.

44 V. Montembault, J. C. Soutif and J. C. Brosse, *React. Funct. Polym.*, 1996, **29**, 29-39.

45 W. S. W. Ngah, C. S. Endud and R. Mayanar, *React. Funct. Polym.*, 2002, **50**, 181-190.

46 R. Schmuhl, H. M. Krieg and K. Keizer, *Water Sa*, 2001, **27**, 1-7.

47 J. C. Y. Ng, W. H. Cheung and G. Mckay, *J. Colloid Interf. Sci.*, 2002, **255**, 64-74.

48 M. Janssoncharrier, E. Guibal, J. Roussy, B. Delanghe and P. Lecloirec, *Water Res.*, 1996, **30**, 465-475.

49 M. R. Gandhi and S. Meenakshi, *J. Hazard. Mater.*, 2012, **203**, 29-37.

50 R. Singhon, J. Husson, M. Knorr, B. Lakard and M. Euvrard, *Coll. Surf. B*, 2012, **93**, 1-7.

51 D. T. Sawyer, *Ann. N. Y. Acad. Sci.*, 1960, **88**, 307-321.

52 K. Binnemans and C. Gorller-Walrand, *J. Rare Earths*, 1996, **14**, 173-180.

53 R. M. Supkowski and W. D. Horrocks, *Inorg. Chim. Acta*, 2002, **340**, 44-48.

54 W. D. Horrocks and D. R. Sudnick, *J. Am. Chem. Soc.*, 1979, **101**, 334-340.

55 R. H. Byrne and B. Q. Li, *Geochim. Cosmochim. Acta*, 1995, **59**, 4575-4589.

56 D. A. Skoog, D. M. West and F. J. Holler, *Fundamentals of analytical chemistry, 7th Edition*, Saunders College Publishers, Philadelphia, 1996.

57 F. V. Pereira, L. V. A. Gurgel and L. F. Gil, *J. Hazard. Mater.*, 2010, **176**, 856-863.

58 K. Binnemans, P. T. Jones, B. Blanpain, T. Van Gerven, Y. Yang, A. Walton and M. Buchert, *J. Clean. Prod.*, 2013, **51**, 1-22.

59 C. K. Gupta and N. Krishnamurthy, *Int. Mater. Rev.*, 1992, **37**, 197-248.

60 Z. S. Yu and M. B. Chen, *Rare Earth Elements and their Applications*, Metallurgical Industry Press, Beijing (P.R. China), 1995.

Figure captions

Figure 1. Structures of EDTA-functionalized chitosan (left) and DTPA-functionalized chitosan (right).

Figure 2. Emission spectrum of an europium(III)-EDTA-chitosan complex (λ_{exc} = 395 nm, room temperature).

Figure 3. Influence of contact time on the adsorbed amount of Nd^{3+} (aqueous feed concentration: 200 ppm).

Figure 4: Effect of initial Nd^{3+} ion concentration on the adsorption performance of modified and unmodified chitosan.

Figure 5: Influence of equilibrium pH on the amount of Nd^{3+} adsorbed by EDTA-chitosan and DTPA-chitosan.

Figure 6: DTPA-chitosan distribution coefficient for some lanthanides as a function of equilibrium pH.

Figure 7: Selective adsorption amount for DTPA-chitosan as a function of equilibrium pH.

Figure 8: Enrichment of Dy^{3+} in comparison to Nd^{3+} (1:1 molar ratio) as a function of the equilibrium pH.

Figure 9: Chromatogram Nd^{3+}/Ho^{3+} separation (1:1 mass ratio) with DTPA-chitosan/silica at pH 1.

Figure 10: Breakthrough curve for Nd^{3+}/Ho^{3+} separation (1:1 mass ratio) with DTPA-chitosan/silica at pH 1.25.

Figure 11: Chromatogram for the separation of a $Pr^{3+}/Nd^{3+}/Ho^{3+}$ mixture (ratio 1:1:1) with DTPA-chitosan/silica

Figure 1

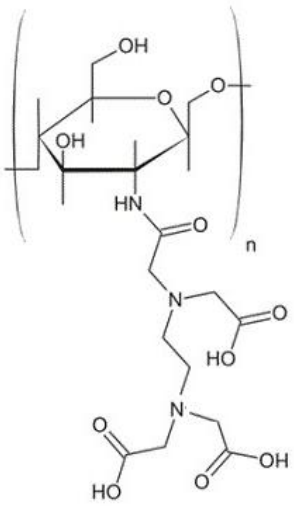

EDTA-chitosan

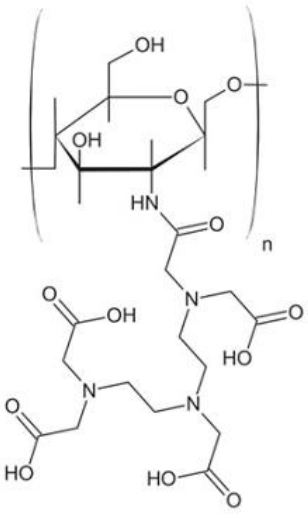

DTPA-chitosan

Figure 2.

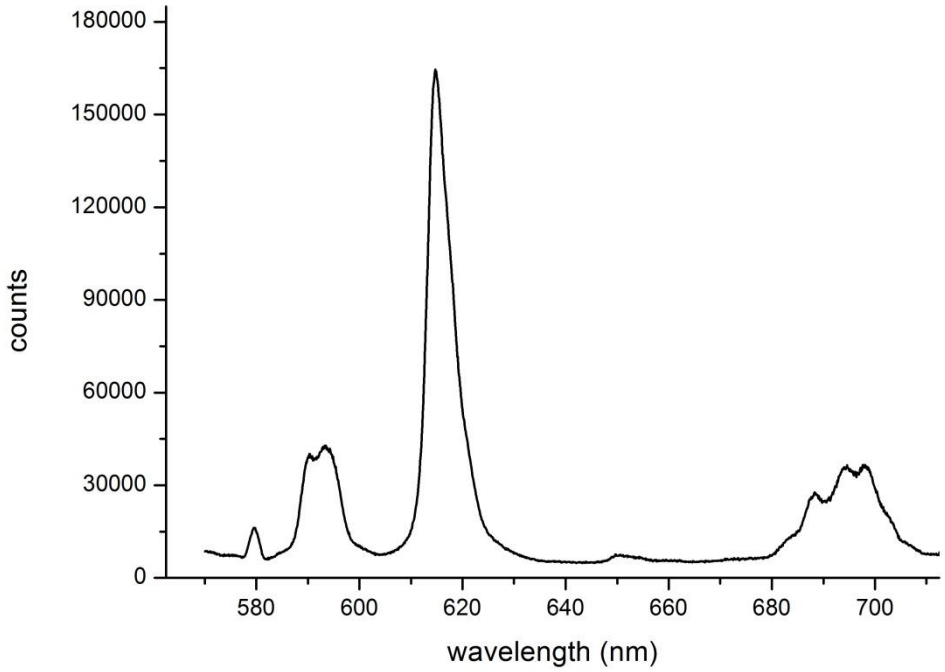
180000
150000
120000
90000
60000
30000
0
counts
580
600
620
640
660
680
700
wavelength (nm)

Figure 3.

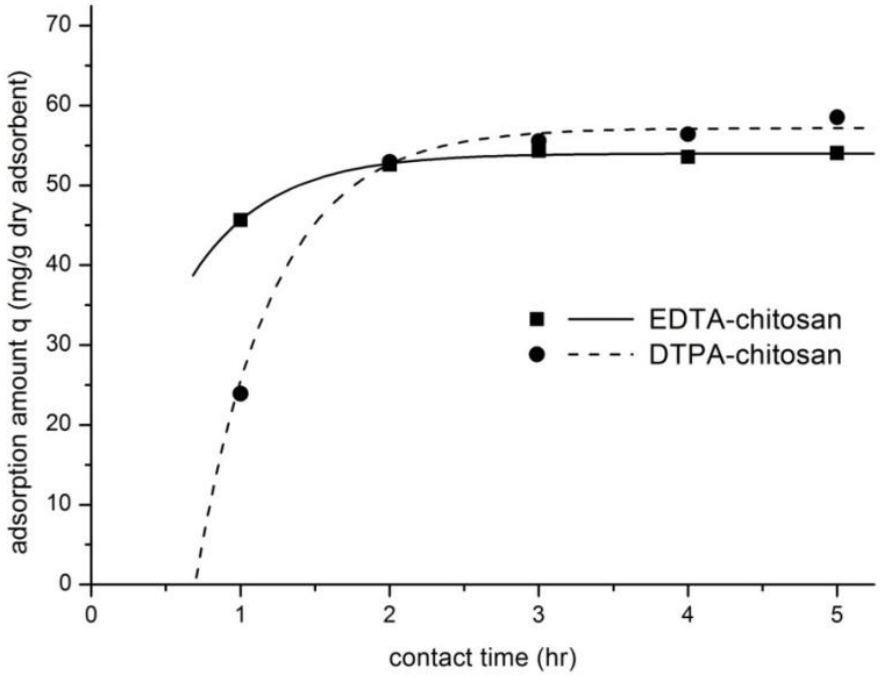
adsorption amount q (mg/g dry adsorbent)
contact time (hr)
EDTA-chitosan
DTPA-chitosan
0
10
20
30
40
50
60
70
0
1
2
3
4
5

Figure 4.

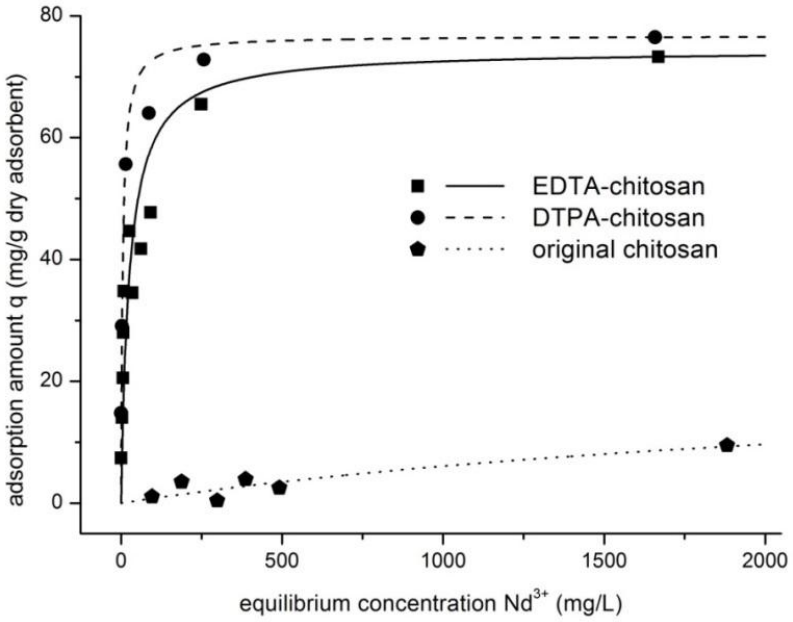
adsorption amount q (mg/g dry adsorbent)
equilibrium concentration Nd3+ (mg/L)
EDTA-chitosan
DTPA-chitosan
original chitosan
0
20
40
60
80
0
500
1000
1500
2000

Figure 5.

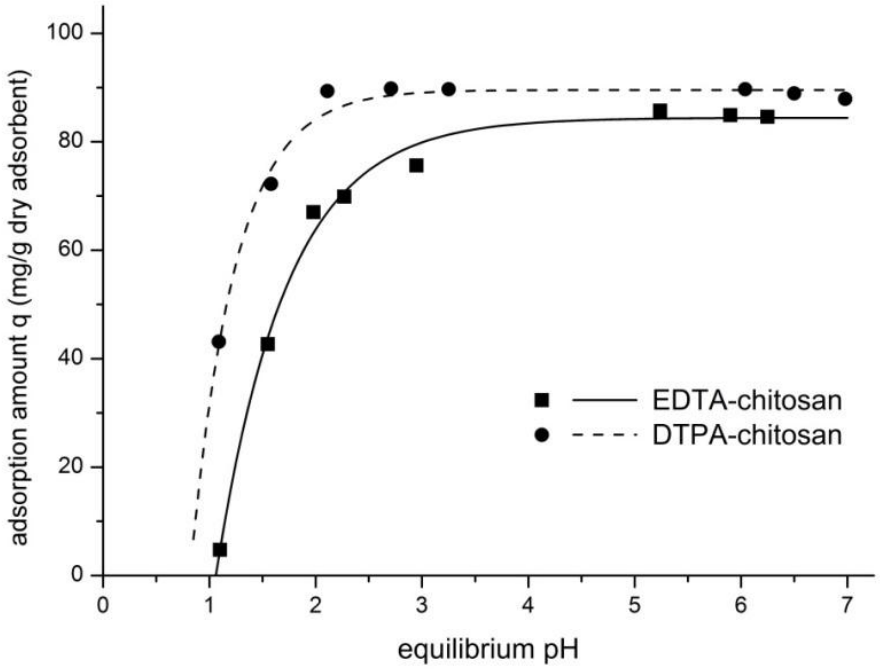
adsorption amount q (mg/g dry adsorbent)
equilibrium pH
EDTA-chitosan
DTPA-chitosan
0
20
40
60
80
100
0
1
2
3
4
5
6
7

Figure 6.

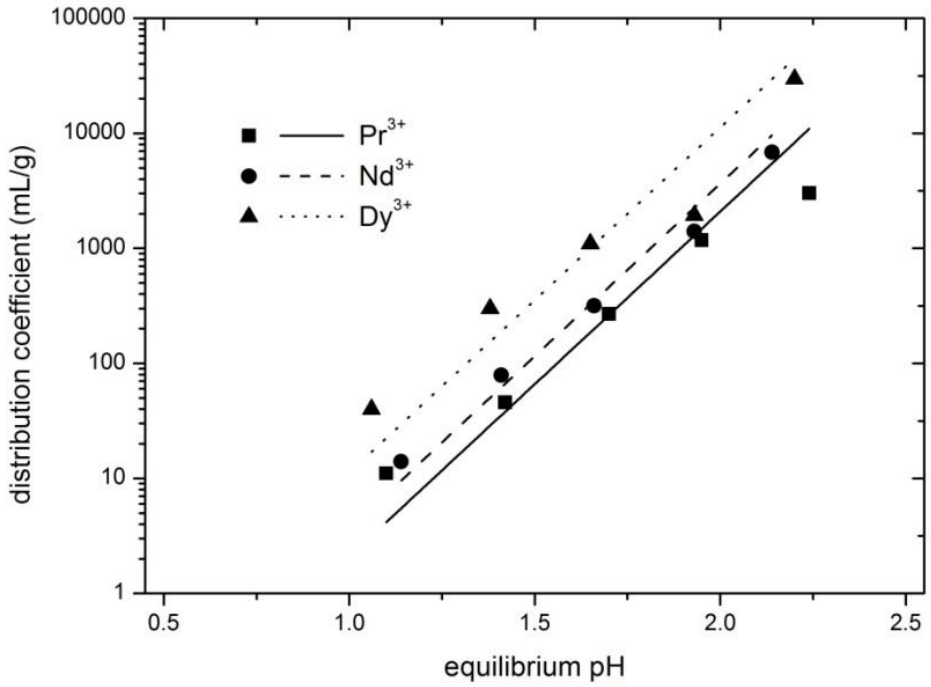
distribution coefficient (mL/g)
100000
10000
1000
100
10
1
0.5
1.0
1.5
2.0
2.5
equilibrium pH
Pr3+
Nd3+
Dy3+

Figure 7.

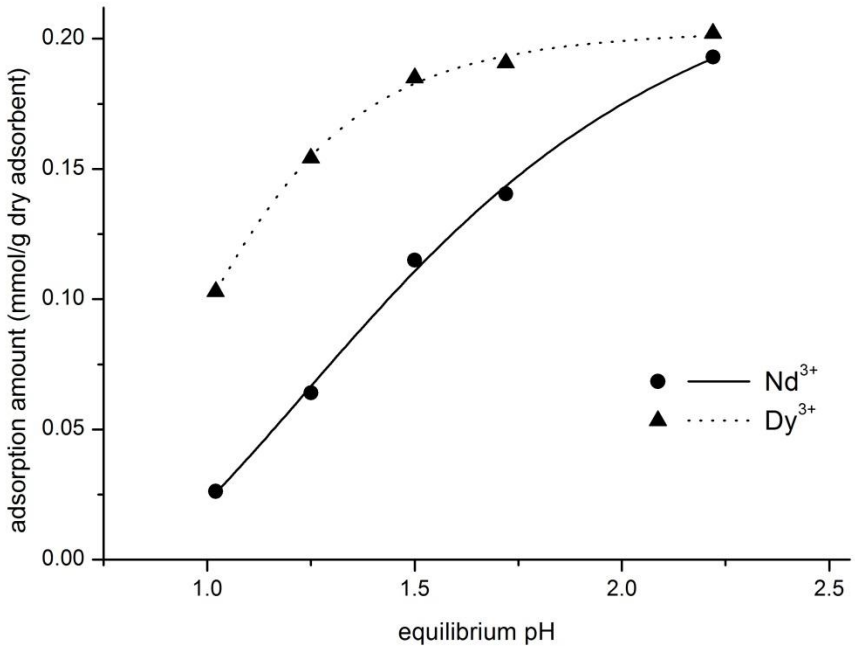
adsorption amount (mmol/g dry adsorbent)
0.00
0.05
0.10
0.15
0.20
1.0
1.5
2.0
2.5
equilibrium pH
Nd3+
Dy3+

Figure 8.

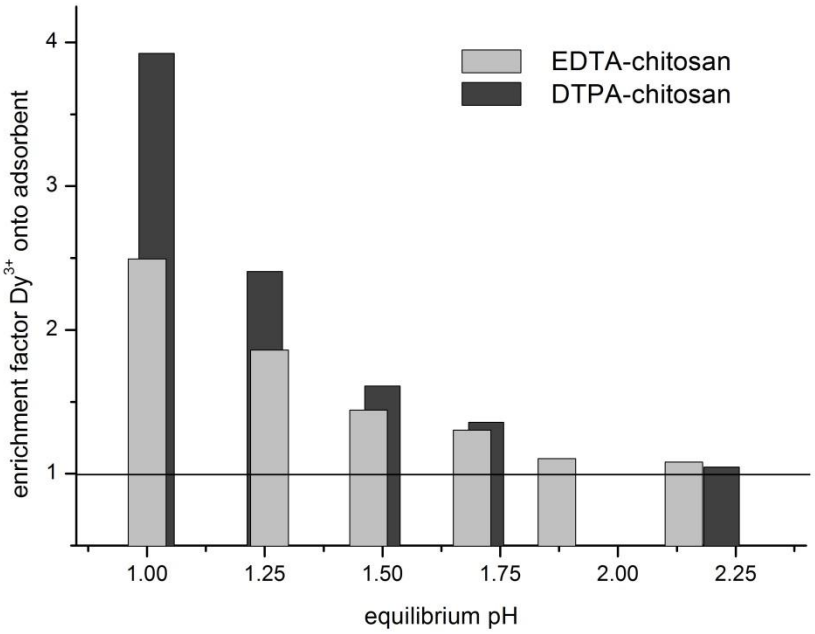
EDTA-chitosan
DTPA-chitosan
enrichment factor Dy^{3+} onto adsorbent
4
3
2
1
1.00
1.25
1.50
1.75
2.00
2.25
equilibrium pH

Figure 9.

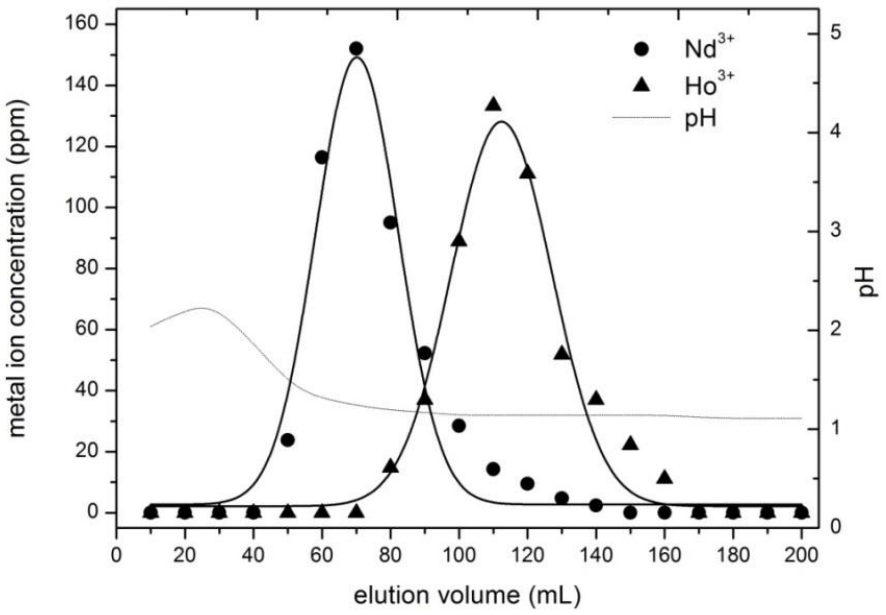
metal ion concentration (ppm)
elution volume (mL)
pH
Nd3+
Ho3+
pH
0
20
40
60
80
100
120
140
160
180
200
0
1
2
3
4
5

Figure 10.

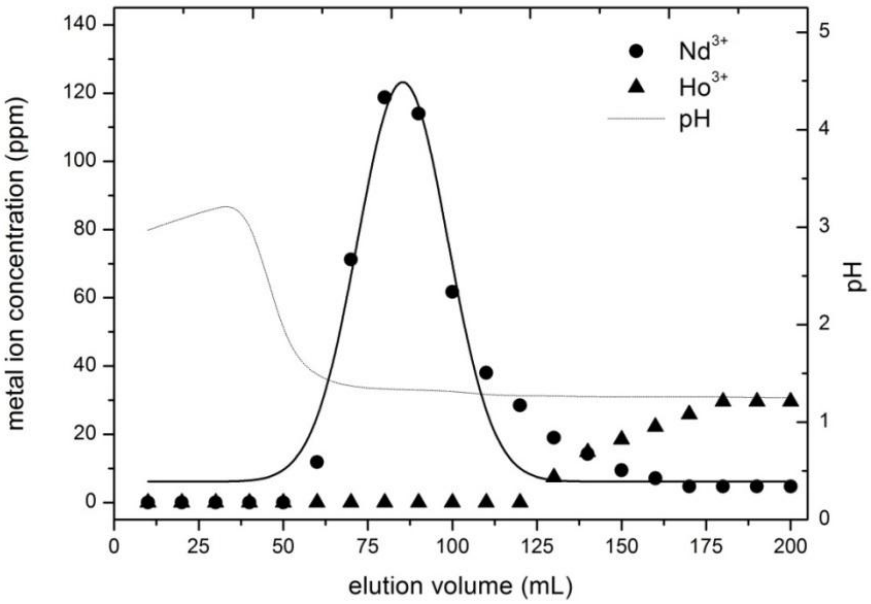
metal ion concentration (ppm)
elution volume (mL)
pH
Nd3+
Ho3+
pH
0
20
40
60
80
100
120
140
0
25
50
75
100
125
150
175
200
0
1
2
3
4
5

Figure 11.

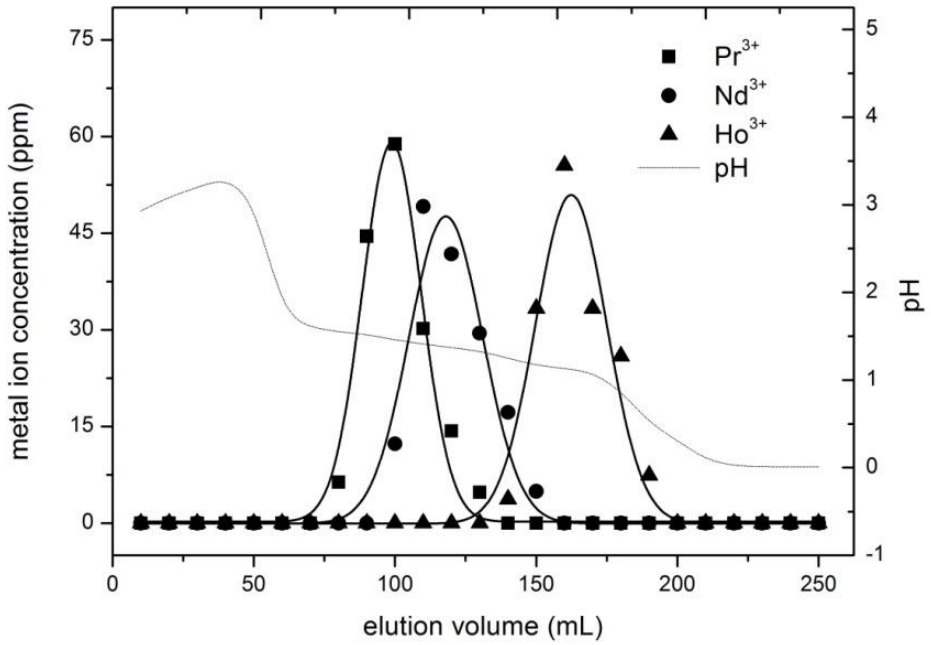
metal ion concentration (ppm)
elution volume (mL)
pH
Pr3+
Nd3+
Ho3+
pH
0
15
30
45
60
75
0
50
100
150
200
250
-1
0
1
2
3
4
5

.